articles

molecular pharmaceutics

Influence of Charge and Steric Bulk in the C-24 Region on the Interaction of Bile Acids with Human Apical Sodium-Dependent Bile Acid Transporter

Anand Balakrishnan,[†,‡] Stephen A. Wring,[§] Andrew Coop,[†] and James E. Polli*[,†]

Department of Pharmaceutical Sciences, School of Pharmacy, University of Maryland, Baltimore, Maryland 21201, and Trimeris Inc., Morrisville, North Carolina 27560

Received February 8, 2006

Abstract: The human apical sodium-dependent bile acid transporter (hASBT) is a potential target for drug delivery, but an understanding of hASBT substrate requirements is limited. The objective of this study was to evaluate the influence of ionic character and steric bulk in the C-24 region of bile acid conjugates in governing interaction with hASBT. Ionic character was studied using chenodeoxycholate (CDCA) conjugates of glutamic acid and lysine, which varied in charge (monoanionic, dianionic, cationic, neutral, and zwitterionic) and location of charge (proximal or distal to C-24). Steric effects were evaluated using ester conjugates that varied in ester substituent size (methyl, benzyl, and *tert*-butyl) and location (proximal and/or distal). Conjugate interaction with hASBT was assessed via transport and inhibition studies, using a hASBT-MDCK monolayer. Monoanionic, cationic, and neutral conjugates of CDCA exhibited high inhibitory potency (K_i < 10 μM). High inhibition potency of neutral and cationic conjugates indicated that a negative charge is not essential for hASBT binding. Dianionic conjugates exhibited low inhibition potency (K_i > 100 μM). Conjugates with a single bulky ester substituent proximal or distal to the C-24 region exhibited high inhibition potency. However, two bulky substituents practically abolished interaction. In transport studies, monoanionic conjugates were high affinity hASBT substrates. Meanwhile, cationic and zwitterionic conjugates were not substrates for hASBT. Overall, C-24 ionic character influenced interaction with hASBT. Although the presence of a single negative charge was not essential for interaction with hASBT, monoanionic conjugates were favored for hASBT-mediated transport compared to cationic and zwitterionic conjugates.

Keywords: Bile acids; prodrugs; hASBT; QSAR; SLC10A2; cell culture; transporters

Introduction

The bioavailability of oral drug candidates is often limited by their low intestinal permeability. Intestinal permeability of drugs can be enhanced via a prodrug approach targeting influx transporters in the small intestine. hASBT is a member of the solute carrier (SLC) genetic superfamily and is an attractive target for prodrug targeting, given its high transport capacity. As is often the case with transport targeted delivery,[1] native substrates (i.e., bile acids for hASBT) have been employed as targeting moieties.[2] Coupling of the drug

* Author to whom correspondence should be addressed. Mailing address: Department of Pharmaceutical Sciences, School of Pharmacy, University of Maryland, HSF2, room 623, Baltimore, MD 21201. Tel: 410-706-8292. Fax: 410-706-5017. E-mail: jpolli@rx.umaryland.edu.

† University of Maryland.

‡ Current address: Merck & Co., Inc., West Point, PA 19486.

§ Trimeris Inc.

(1) Steffansen, B.; Nielsen, C. U.; Frokjaer, S. Delivery aspects of small peptides and substrates for peptide transporters. *Eur. J. Pharm. Biopharm.* **2005**, *60*, 241−245.

(2) Tolle-Sander, S.; Lentz, K. A.; Maeda, D. Y.; Coop, A.; Polli, J. E. Increased acyclovir oral bioavailability via a bile acid conjugate. *Mol. Pharm.* **2004**, *1*, 40−48.

10.1021/mp0600135 CCC: $33.50
Published on Web 04/29/2006

to the bile acid could be via the bile acid's C-24 carboxylate or the C-3 hydroxyl group.[3−5] For example, a 2-fold enhancement in acyclovir bioavailability was achieved in rats, when acyclovir was C-24 conjugated to CDCA via a valine linker.[2]

The lack of knowledge of hASBT substrate requirements has impeded progress in rational prodrug design targeting hASBT. In particular, the influence of C-24 chemistry space in enhancing or impeding the interaction of bile acid analogues with hASBT is not clear. Previous studies have indicated that steroidal hydroxylation patterns and C-24 conjugation patterns govern the interaction of native bile acids with hASBT.[6] It was observed that conjugation at C-24 enhanced inhibition potency and transport affinity of bile acids to hASBT. Additionally, it was reported that the C-24 region dominated steroidal hydroxylation effects in certain bile acids. These studies provide insight into structural features of the targeting moiety (i.e., bile acid) that favor interaction with hASBT. However, it is not clear how C-24 chemistry influences interaction with hASBT.

Lack et al. proposed that a negative charge around the C-24 region is essential for interaction with hASBT.[7] This observation also reflects that all the native bile acids carry a negative charge in the C-24 region. Most previous studies have focused on compounds incorporating a negative charge around C-24. For example, Swaan and colleagues examined the transport of four C-24 bile acid conjugates across Caco-2 monolayers.[5] Each provided a negative charge near C-24. Two conjugates were rapidly transported. Subsequent QSAR analysis suggested that the C-24 side chain can be 14 Å in length or longer for translocation, and that large hydrophobic moieties increase binding to hASBT.[8] Previous studies from our laboratory with neutral acyclovir conjugates indicate that neutral conjugates are transported via hASBT. The same observation was also made by Swaan et al., suggesting that a hydrogen bond acceptor could substitute for the negative charge.[8]

The objective of this study was to evaluate the influence of ionic character and steric bulk around the C-24 region of bile acid conjugates in governing interaction with hASBT. Ionic character was studied using chenodeoxycholate conjugates of glutamic acid or lysine. Conjugates varied in the nature of charge (monoanionic, dianionic, cationic, neutral, and zwitterionic) and location of charge (proximal or distal to C-24). Steric effects were evaluated using conjugates of lysine or glutamate that varied in substituent bulkiness and location of the bulky substituent (proximal and/or distal). Additionally, these also provide scaffolding for the subsequent attachment of potential drug candidates, directly extending these results to potential prodrug design. Requirements for hASBT inhibition can be expected to differ from requirements for hASBT-mediated translocation. Hence, both transport and inhibition studies were performed for each conjugate.

Experimental Section

Materials. Geneticin, fetal bovine serum, trypsin, and DMEM were purchased from Invitrogen Corporation (Carlsbad, CA). [^{3}H]-Taurocholic acid and [^{14}C]-mannitol were purchased from American Radiolabeled Chemicals (St. Louis, MO). Protected glutamate and lysine analogues were obtained from Bachem America (Philadelphia, PA). All other chemicals were obtained from Sigma Chemical (St. Louis, MO) or TCI America (Portland, OR).

Overview of Synthetic Approaches. CDCA conjugates were designed to evaluate the influence of ionic character and steric bulk around the C-24 region. Among the native bile acids, CDCA was selected on the basis of its favorable transport across hASBT-MDCK monolayers. CDCA was conjugated with either glutramate or lysine derivative (Figure 1 and Figure 2, respectively). Since glutamate carries both carboxylate and amine functions, a two-stage indirect coupling approach was selected using an *N*-hydroxysuccinimide ester intermediate of CDCA. This approach was particularly useful for monoanionic glutamic acid conjugates and is illustrated in Figure 3. Neutral conjugates were synthesized via a simple one-step reaction using HBTU as a coupling agent in the presence of triethylamine (TEA) as base. Lysine conjugates were synthesized using orthogonal protection for the ϵ-amine and α-carboxylate, as illustrated in Figure 4.

Synthesis of *N*-Hydroxysuccinimide Ester of CDCA. CDCA (5.89 g, 15 mmol) was dissolved in 30 mL of dry dimethylformamide (DMF), along with 2.3 mL (16.5 mmol) of triethylamine (TEA) and 5.89 g (15.5 mmol) of HBTU at room temperature. *N*-Hydroxysuccinimide (1.9 g, 16.5 mmol) was dissolved in DMF and added dropwise to the above mixture. The mixture was stirred for 4 h at room temperature. The contents were poured into brine and extracted into diethyl ether. The ether extract was washed thrice with cold water and once with 10% sodium carbonate. The ether extract was evaporated under vacuum to yield a fluffy white powder (yield 7.0 g). TLC of the intermediate indicated a single spot (CH_2Cl_2/CH_3OH = 9:1). This intermediate was used in the subsequent synthetic schemes. Mass spectrometry (MS) indicated appropriate peaks: [M + 1] 490.31 and [M + Na]

(3) Kramer, W.; Wess, G. Bile acid transport systems as pharmaceutical targets. *Eur. J. Clin. Invest.* **1996**, *26*, 715−732.
(4) Kullak-Ublick, G. A.; Glasa, J.; Boker, C.; Oswald, M.; Grutzner, U.; et al. Chlorambucil-taurocholate is transported by bile acid carriers expressed in human hepatocellular carcinomas. *Gastroenterology* **1997**, *113*, 1295−1305.
(5) Swaan, P. W.; Hillgren, K. M.; Szoka, F. C., Jr.; Oie, S. Enhanced transepithelial transport of peptides by conjugation to cholic acid. *Bioconjugate Chem.* **1997**, *8*, 520−525.
(6) Balakrishnan, A.; Wring, S. A.; Polli, J. E. Interaction of Native Bile Acids with Human Apical Sodium Dependent Bile Acid Transporter (hASBT): Influence of Steroidal Hydroxylation Pattern and C-24 Conjugation. *Pharm. Res.* **2006**, in press.
(7) Lack, L. Properties and biological significance of the ileal bile salt transport system. *Environ. Health Perspect.* **1979**, *33*, 79−90.
(8) Swaan, P. W.; Szoka, F. C., Jr.; Oie, S. Molecular modeling of the intestinal bile acid carrier: a comparative molecular field analysis study. *J. Comput.-Aided Mol. Des.* **1997**, *11*, 581−588.

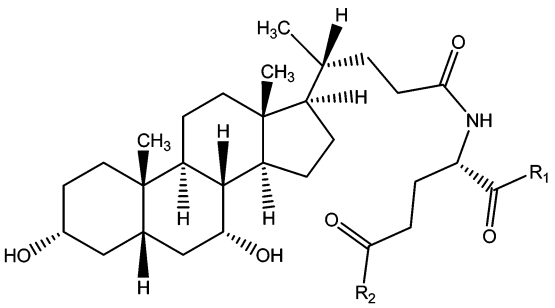

Ionic character	Conjugate[a]	R_1	R_2
Dianionic	Glutamic acid CDCA amide	-OH	-OH
Monoanionic	α methyl glutamic acid CDCA amide	$-OCH_3$	-OH
	γ methyl glutamic acid CDCA amide	-OH	$-OCH_3$
	α benzyl glutamic acid CDCA amide	$-OCH_2C_6H_5$	-OH
	γ benzyl glutamic acid CDCA amide	-OH	$-OCH_2C_6H_5$
Neutral	α, γ dimethyl glutamic acid CDCA amide	$-OCH_3$	$-OCH_3$
	α, γ dibenzyl glutamic acid CDCA amide	$-OCH_2C_6H_5$	$-OCH_2C_6H_5$
	α methyl, γ t-butyl glutamic acid CDCA amide	$-OCH_3$	$OC(CH_3)_3$
	α t-butyl, γ methyl glutamic acid CDCA amide	$OC(CH_3)_3$	$-OCH_3$

[a] CDCA denotes chenodeoxycholate

Figure 1. Glutamate conjugates of CDCA. Conjugates differ with respect to number of negative charge (0, 1, or 2), location of a negative charge (α or γ), and nature of the ester groups (methyl, benzyl, and *tert*-butyl). Glutamic acid CDCA amide carries two negative charges proximal and distal to C-24 (i.e., α and γ positions, respectively). Monoanionic conjugates contained either one proximal or one distal carboxylate, with the other methyl or benzyl esterified. For neutral conjugates, each of the carboxylates was esterified with substituents varying in size.

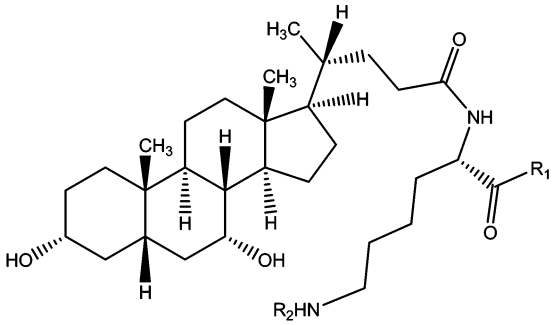

Ionic character	Conjugate[a]	R_1	R_2
Zwitterionic	α lysine CDCA amide	-OH	-H
Cationic	α lysine methyl ester CDCA amide	$-OCH_3$	-H
Neutral	α lysine(CBZ) benzyl ester CDCA amide	$-OCH_3$	$-COOCH_2C_6H_5$

[a] CDCA denotes chenodeoxycholate

Figure 2. Lysine conjugates of CDCA. In contrast to glutamate conjugates, lysine conjugates can provide a positive charge distal to C-24. The three lysine conjugates differed in ionic character. α-Lysine CDCA amide is zwitterionic with an α-carboxylate and ϵ-amino group. α-Lysine methyl ester CDCA amide is a cationic conjugate, since the α-carboxylate is methyl esterified. α-Lysine(CBZ) benzyl ester CDCA amide is neutral, since the α-carboxylate and ϵ-amino group are benzyl esterified and CBZ protected, respectively.

512.31. ^{13}C NMR ($CDCl_3$): δ 11.8, 18.2, 20.6, 22.8, 23.7, 25.6, 28.0, 28.2, 30.7, 32.9, 34.6, 35.1, 35.2, 35.3, 38.7, 39.5, 39.6, 39.9, 41.5, 42.8, 50.5, 55.7, 68.6, 72.1, 75.1, 106.1, 111.2, 117.3, 126.3, 126.7, 169.2, 169.2.

Synthesis of Monoanionic Glutamate Conjugates of CDCA. In the synthesis of α-methyl ester glutamic acid CDCA amide, 3.43 g (7 mmol) of *N*-hydroxysuccinimide ester of CDCA was dissolved in 15 mL of dry dimethylformamide (DMF), along with 1.12 mL (7 mmol) of triethylamine (TEA) at room temperature. α-Methyl glutamic acid (1.13 g, 7 mmol) was dispersed in 8 mL of DMF and added dropwise to the above mixture. The mixture was stirred for

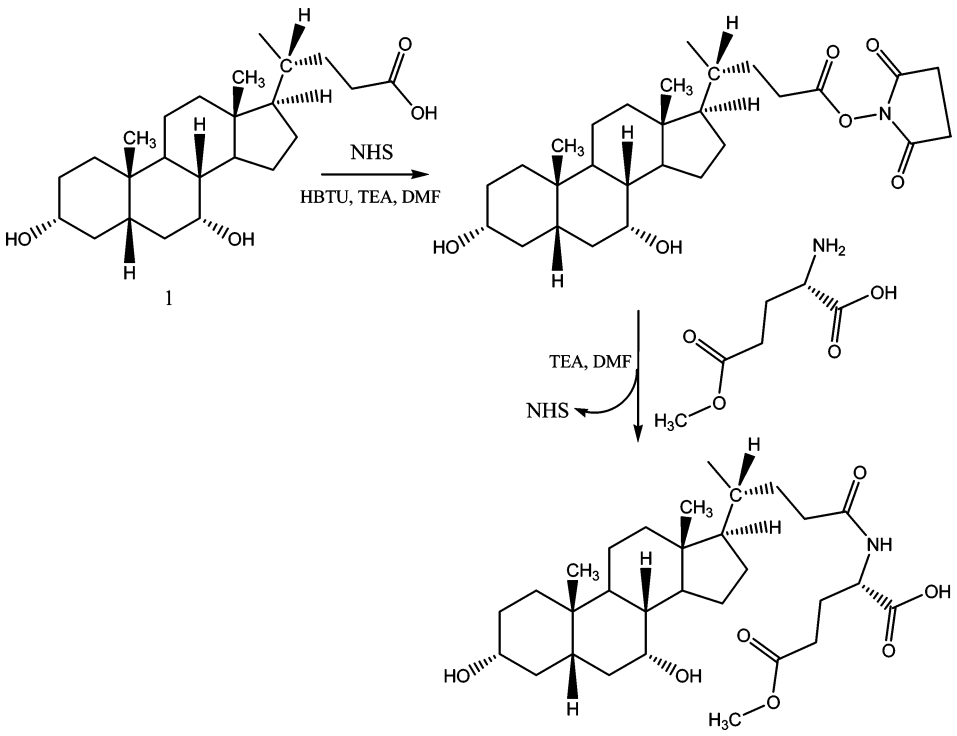

Figure 3. Synthetic scheme for monoanionic conjugates of CDCA. Since glutamate possesses both the carboxylate and amine functions, conjugation to CDCA was carried out via an activated ester approach using the *N*-hydroxysuccinimide (NHS) ester intermediate. The scheme illustrates the synthesis of γ-methyl glutamic acid CDCA amide.

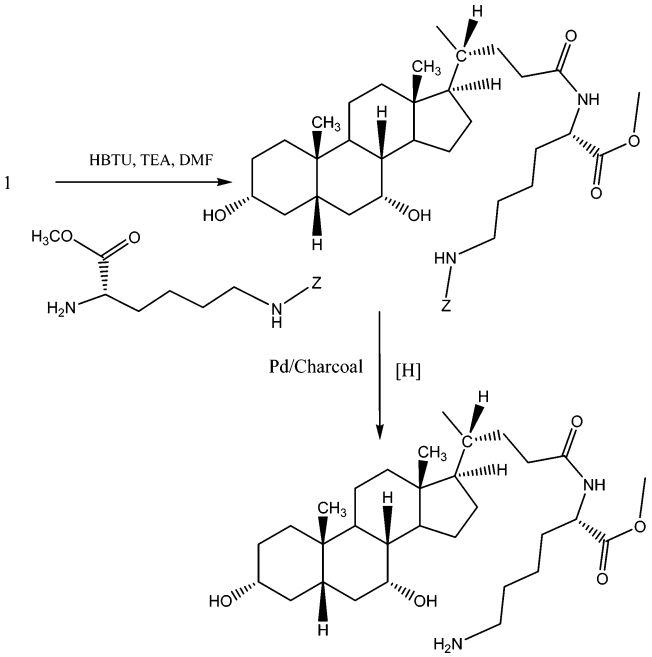

Figure 4. Synthetic scheme for lysine conjugates of CDCA. Each lysine conjugate was synthesized via coupling of a protected lysine derivative to CDCA using HBTU in the presence of TEA. The scheme illustrates the synthesis of α-lysine methyl ester CDCA amide as an example. Subsequent hydrogenation resulted in the generation of the target compound following deprotection.

12 h at room temperature. DMF was evaporated under vacuum at a temperature less than 40 °C. The crude product was dissolved in a mixture of 1:1 methanol and dichloromethane and subsequently adsorbed onto 10 g of dried silica. The crude mixture was loaded on a silica column and eluted with a gradient system from zero to 20% methanol and dichloromethane, along with 1% acetic acid. Fractions were collected, and the solvents were evaporated under vacuum to yield buff colored product. The yield was approximately 90% for crude product; after column purification the yield was 60%. TLC of the final product showed a single spot free of impurities ($CH_2Cl_2/CH_3OH/CH_3COOH$ = 8:2:0.1). MS indicated appropriate peaks: [M + 1] 536.35, [M + Na] 558.35, and [M − 1] 534.35. ^{13}C NMR ($CDCl_3$): δ 11.8, 18.5, 20.6, 22.8, 23.7, 27.5, 28.3, 30.2, 30.6, 31.0, 31.2, 32.8, 34.6, 35.1, 35.4, 36.6, 39.4, 39.7, 41.5, 42.7, 50.5, 51.8, 55.5, 67.5, 68.6, 72.1, 128.3, 128.6, 128.7, 135.1, 162.7, 172.0, 174.2, 175.7.

The synthesis of the γ-methyl ester glutamic acid CDCA amide was performed in a similar fashion. TLC of the final product showed a single spot free of impurities ($CH_2Cl_2/CH_3OH/CH_3COOH$ = 8:2:0.1). MS indicated appropriate peaks: [M + 1] 536.35, [M + Na] 558.35, and [M − 1] 534.35. ^{13}C NMR ($(CD_3)_2SO$): δ 21.6, 23.2, 23.7, 26.8, 28.3, 30.3, 31.1, 32.0, 32.6, 32.8, 35.3, 35.3, 35.5, 35.8, 39.5, 39.6, 39.9, 40.3, 40.4, 40.6, 41.9, 42.4, 50.5, 51.5, 51.9, 56.1, 66.7, 70.8, 173.2,173.3, 173.8.

α-Benzyl ester glutamic acid CDCA amide and γ-benzyl ester glutamic acid CDCA amide were each synthesized in a similar fashion via the *N*-hydroxysuccinimide intermediate. After evaporation of DMF, residue was dissolved in 50 mL of dichloromethane and washed five times with 50 mL of

water. The DCM extract was subsequently dried using brine and sodium sulfate. Removal of DCM under vacuum yielded the compound as a buff colored precipitate, with 80% product yield. TLC of the final product showed a single spot free of impurities (CH_2Cl_2/CH_3OH = 8:2). MS indicated appropriate peaks: [M + 1] 612.39 and [M − 1] 610.38. For α-benzyl ester glutamic acid CDCA amide: ^{13}C NMR (CD_3Cl) δ 11.8, 18.4, 20.6, 22.8, 23.7, 27.4, 28.2, 30.2, 30.6, 31.4, 32.9, 34.6, 35.1, 35.4, 39.4, 39.7, 40.8, 41.5, 42.7, 50.4, 51.8, 55.5, 67.4, 68.6, 72.1, 76.6, 102.1, 128.3, 128.6, 128.7, 135.2, 172.0, 174.2, 175.6. For γ-benzyl ester glutamic acid CDCA amide: ^{13}C NMR (CD_3Cl) δ 11.8, 18.4, 20.6, 22.8, 23.7, 26.7, 28.3, 30.6, 31.6, 32.9, 33.1, 34.5, 35.1, 35.4, 35.4, 36.6, 39.4, 39.7, 41.5, 42.7, 50.4, 52.2, 55.7, 65.4, 66.8, 68.6, 72.1, 127.0, 127.7, 128.3, 128.4, 128.6, 128.7, 135.6, 155.4, 162.8, 173.5, 173.6, 174.9.

Synthesis of Neutral Glutamate Conjugates of CDCA. In the synthesis of α,γ-dimethyl ester glutamic acid CDCA amide, 1.57 g (4 mmol) of CDCA was dissolved in 10 mL of dry DMF, along with 0.5 mL (4 mmol) of TEA at room temperature. α,γ-Dimethyl glutamic acid (1.06 g, 5 mmol) was dissolved in 7 mL of dry DMF and added to the above mixture and stirred for 6 h at room temperature. The crude mixture was poured into ice cold distilled water and extracted into diethyl ether. The ether extract was washed thrice with water and once with brine. The crude mixture was loaded on a silica column and eluted with a gradient solvent system ranging from zero to 10% methanol in dichloromethane. Fractions were collected, and the solvents were evaporated under vacuum. The yield was approximately 90% for crude product; after column purification the yield was 80%. TLC of the final product showed a single spot free of impurities (CH_2Cl_2/CH_3OH = 9:1). MS indicated appropriate peaks: [M + 1] 550.37 and [M + Na] 572.37. ^{13}C NMR ($CDCl_3$): δ 12.0, 18.6, 20.8, 23.0, 23.9, 27.6, 28.4, 30.3, 30.9, 31.7, 33.0, 33.5, 34.8, 35.3, 35.5, 35.7, 39.6, 39.8, 40.1, 41.7, 42.9, 50.7, 51.8, 52.1, 52.8, 56.0, 68.7, 72.3, 172.7, 173.6, 173.8.

The syntheses of α-*tert*-butyl, γ-methyl glutamic acid CDCA amide and γ-*tert*-butyl, α-methyl glutamic acid CDCA amide were performed in a similar fashion. TLC showed a single spot free of impurities for each of the compounds (CH_2Cl_2/CH_3OH = 9:1). MS indicated appropriate peaks for each: [M + 1] 592.41 and [M + Na] 614.41. For γ-methyl, α-*tert*-butyl glutamic acid CDCA amide: ^{13}C NMR ($CDCl_3$) δ 11.8, 18.7, 20.6, 22.8, 23.7, 27.7, 28.1, 28.2, 30.7, 30.9, 31.5, 31.6, 32.8, 33.4, 34.6, 35.1, 35.3, 35.1, 35.5, 39.7, 39.9, 41.5, 42.7, 50.5, 51.7, 52.5, 55.9, 68.5, 72.0, 80.9, 95.2, 172.3, 177.7, 173.5. For α-methyl γ-*tert*-butyl glutamic acid CDCA amide: ^{13}C NMR ($CDCl_3$) δ 11.8, 18.4, 20.6, 22.8, 23.7, 27.3, 28.1, 28.2, 30.7, 31.0, 31.5, 32.9, 33.4, 34.6, 35.1, 35.4, 35.5, 39.5, 39.7, 39.9, 41.5, 42.8, 50.5, 51.8, 52.5, 55.9, 68.6, 72.1, 80.9, 172.4, 172.7, 173.5.

α,γ-Dibenzyl glutamic acid CDCA amide was synthesized in a similar fashion and purified via extraction. MS indicated appropriate peaks: [M + 1] 702.43 and [M + Na] 724.41. ^{13}C NMR ($CDCl_3$): δ 3.0, 15.9, 19.0, 23.5, 34.7, 36.8, 38.0, 45.7, 47.0, 61.9, 63.9, 67.3, 123.6, 130.4, 131.0, 167.2, 168.0, 168.9.

Synthesis of Dianionic Glutamate Conjugate of CDCA. For the synthesis of glutamic acid CDCA amide, α,β-dibenzyl ester glutamic acid CDCA amide was dissolved in methanol and subjected to catalytic hydrogenation, using 10% palladium on charcoal in a Parr apparatus overnight. Caution must be exercised during the addition of Pd/charcoal into methanol, as the mixture may ignite. The mixture was subsequently filtered over a layer of Celite. Methanol was evaporated under vacuum to yield the target compound as a white precipitate with 90% product yield. TLC of the final product showed a single spot free of impurities ($CH_2Cl_2/CH_3OH/CH_3COOH$ = 8:2:1). MS indicated an appropriate peak under the negative ion mode: [M − 1] 520.34. ^{13}C NMR (CD_3OH): δ 9.3,16.0, 18.9, 20.5, 21.7, 25.0, 26.5, 28.4, 28.4, 30.3, 30.9, 31.1, 33.0, 33.3, 33.6, 33.9, 37.6, 37.9, 38.2, 40.3, 40.8, 41.7, 43.8, 45.9, 48.1, 48.6, 50.1, 54.5, 66.2, 70.0, 172.2, 173.4, 174.0.

Synthesis of Lysine Conjugates of CDCA. In the synthesis of α-lysine(CBZ) benzyl ester CDCA amide, 1.96 g (5 mmol) of CDCA was dissolved in 15 mL of dry DMF, along with 1.2 mL (6 mmol) of TEA at room temperature. Lysine(CBZ) benzyl ester (2.40 g, 6 mmol) was dissolved in 7 mL of dry DMF and added to the above mixture and stirred for 6 h at room temperature. The crude mixture was poured into ice cold distilled water and extracted into diethyl ether. The ether extract was washed thrice with water and once with brine. The ether extract was dried using sodium sulfate and evaporated under vacuum to yield a buff colored precipitate of α-lysine(CBZ) benzyl ester CDCA amide. The yield exceeded 90%. TLC of this product showed a single spot free of impurities (CH_2Cl_2/CH_3OH = 9:1). MS indicated appropriate peaks: [M + 1] 745.47 and [M + Na] 767.47. ^{13}C NMR (CD_3Cl): δ 11.7, 18.3, 20.5, 22.2, 22.7, 23.6, 28.2, 29.3, 30.6, 31.5, 31.9, 32.8, 34.5, 35.0, 35.3, 39.4, 39.6, 39.8, 40.5, 41.4, 42.6, 50.4, 51.9, 55.6, 66.6, 67.2, 68.5, 72.0, 128.0, 128.3, 128.5, 128.6, 135.3, 136.5, 156.6, 172.4, 173.8.

For the synthesis of α-lysine CDCA amide, α-lysine(CBZ) benzyl ester CDCA amide was dissolved in methanol and subjected to catalytic hydrogenation using 10% palladium on charcoal in a Parr apparatus overnight. Caution must be exercised during the addition of Pd/charcoal into methanol as the mixture may ignite. The mixture was subsequently filtered over a layer of Celite, and methanol was evaporated under vacuum to yield α-lysine CDCA amide as a white precipitate (90% product yield). TLC of the final product showed a single spot free of impurities ($CH_2Cl_2/CH_3OH/CH_3COOH$ = 8:2:1) MS indicated an appropriate peak under the positive ion mode: [M + 1] 521.34.

To synthesize α-lysine methyl ester CDCA amide, lysine-(CBZ) methyl ester was coupled with CDCA in a fashion similar to that described above to yield α-lysine(CBZ) CDCA amide, which was subsequently subjected to catalytic hydrogenation yielding target. Deprotection of the terminal amine group was done via hydrogenation, since the methyl

ester is stable to hydrogenation. CBZ chemistry was chosen over t-boc or f-moc chemistry for deprotection since deprotection using TFA resulted in acylation of the steroidal hydroxyl groups. CBZ was removed conveniently via catalytic hydrogenation using Pd/charcoal. ^{13}C NMR (CD_3-Cl): δ 8.5, 15.8, 18.0, 19.7, 20.2, 20.3, 20.9, 24.5, 25.5, 27.6, 28.2, 29.9, 30.3, 32.2, 32.5, 32.8, 33.2, 36.7, 37.0, 37.3, 39.4, 39.9, 40.9, 43.0, 45.1, 65.3, 69.1, 170.2, 173.2.

Identity of conjugates was confirmed via ^{13}C NMR and MS. ^{13}C NMR spectra contained peaks consistent with the amide linkage and appropriate carbonyl chemistry. MS data was consistent with the desired structures and a lack of bile acid in final product. Purity was assessed by TLC, NMR, and LC−MS. TLC and NMR indicated high levels of purity. Conventional HPLC analysis with UV detection was not suitable for purity evaluations since bile acids do not possess a strong chromophore. Therefore, TLC and NMR were utilized for purity assessment. As an additional measure, CDCA levels in all the products were carefully monitored as the presence of CDCA impurity in the final product can bias results due to its potent interaction with hASBT. The level of CDCA impurity in each conjugate was quantified using LC−MS and was observed to be less than 0.2%.

Cell Culture. Stably transfected hASBT-MDCK cells were cultured as described previously.[9] Briefly, cells were grown at 37 °C, 90% relative humidity, and 5% CO_2 atmosphere and fed every 2 days. Media comprised DMEM supplemented with 10% FBS, 50 units/mL penicillin, and 50 μg/mL streptomycin. Geneticin was used at 1 mg/mL to maintain selection pressure. Cells were passaged every 4 days or after reaching 90% confluence.

Chemical and Metabolic Stability. Conjugates were evaluated for chemical stability in transport buffer for 3 h. Metabolic stability in the presence of cells was evaluated using sodium-free buffer. Conjugates were dissolved in sodium-free buffer (5 μM) and subsequently incubated with cells grown in 12 well plates at 37 °C at 50 rpm. Samples were collected at 15, 30, and 60 min and frozen immediately after the addition of acetonitrile (20% of total volume). Samples were analyzed by LC−MS as described below under analytical methods.

Transport across hASBT-MDCK Monolayers. Transport studies were performed to yield kinetic data that relates to the binding and subsequent translocation across the membrane. hASBT-MDCK cells were grown on polyester Transwells as described earlier.[9] Briefly, cells were seeded at a density of 0.75×10^6 cells/cm^2 on polyester Transwells (Corning; Corning, NY, 0.4 μm pore size, 1 cm^2) and grown as described above. Cells were washed thrice with HBSS or modified HBSS prior to transport study. Studies were carried out at 37 °C at 50 rpm using an orbital shaker. Transport buffer consisted of either Hanks balanced salt solution (HBSS, pH = 6.8), which contains 137 mM NaCl, or a sodium-free, modified HBSS (pH = 6.8) where sodium chloride was replaced with 137 mM tetraethylammonium chloride. Since bile acid transport is sodium-dependent, studies using sodium-free buffer allowed for the measurement of passive transport of bile acids.

Kinetics of hASBT-mediated transport was assessed from transport studies employing a range of donor concentrations for each conjugate. In all studies, [^{14}C]-mannitol was used to monitor monolayer integrity in parallel wells. Mannitol permeability was always less than 2.5×10^{-6} cm/s in each individual well indicating monolayer integrity. The apical and basolateral volumes were 0.5 mL and 1.5 mL, respectively. Samples were quantified using LC−MS and a liquid scintillation counter. Stability of conjugates was monitored during the course of the study via LC−MS and observed to be stable with less than 5% metabolized during the course of the study.

Inhibition Studies. hASBT-MDCK cells were seeded at a density of 1.5×10^6 cells/well in 12 well plates (Corning; Corning, NY) and induced with 10 mM sodium butyrate for 12−15 h at 37 °C prior to study on day 4. Kinetics of hASBT-mediated taurocholate uptake into hASBT-MDCK cells was measured as described earlier.[9] Briefly, cells were washed thrice with HBSS (pH = 6.8) or modified HBSS (pH = 6.8) and incubated with donor solutions at 37 °C and 50 rpm for 10 min. The donor solution was removed, and the cells were washed three times with chilled sodium-free buffer. Cells were lysed using 0.25 mL of 1 N NaOH and neutralized with 0.25 mL of 1 N HCl. Cell lysate was then counted for associated radioactivity using a liquid scintillation counter.

To characterize requirements for hASBT binding, cis-inhibition studies of taurocholate uptake were carried out using individual chenodeoxycholate (CDCA) conjugates at various concentrations (0−100 μM). Taurocholate was used as the substrate. Cells were exposed to donor solution containing taurocholate and CDCA conjugate for 10 min at 37 °C and 50 rpm. After 10 min, the donor solution was removed and the cells were washed three times with chilled sodium-free buffer. Cells were lysed using 0.25 mL of 1 N NaOH and neutralized with 0.25 mL of 1 N HCl. Cell lysate was then counted for associated radioactivity (i.e., taurocholate) using a liquid scintillation counter. Inhibition data was analyzed in terms of the inhibition constant K_i, as described below.

Analytical Methods. Conjugates were analyzed by LC−MS or LC−MS−MS on an Agilent HPLC system, equipped with an autosampler (CTC Analytics, Switzerland) and Applied Biosystems Sciex API4000-Qtrap mass spectrometer. The column was a Phenomenex Luna C18 50 × 2 mm 3μ, heated to 40 °C. The flow rate was 0.7 mL/min. A 3 min gradient was employed using acetonitrile and 10 mM ammonium acetate (pH = 6.8). The gradient mixture started with 1% acetonitrile and terminated with 70% acetonitrile. Detection was achieved under negative ion electrospray tandem mass spectrometry using the [M$^-$] peak for all the

(9) Balakrishnan, A.; Sussman, D. J.; Polli, J. E. Development of stably transfected monolayer overexpressing the human apical sodium-dependent bile acid transporter (hASBT). *Pharm. Res.* **2005**, *22*, 1269−1280.

anionic bile acids, as the [M^-] peak provided the greatest sensitivity. Neutral glutamate conjugates and lysine conjugates were detected under the positive ion mode based on higher sensitivity. Samples were also monitored for metabolites. Radiolabeled taurocholate and mannitol were quantified using a Beckman liquid scintillation counter model LS 5801 (Beckman Instruments; Fullerton, CA) in Econosafe scintillation cocktail.

Data Analysis. Flux data was analyzed as described earlier.[10] This previous study indicated that high transporter expression can lower monolayer resistance, resulting in ABL-limited transport of solutes, leading to biased kinetic estimates if ABL is not considered. The extent of bias is determined by transporter expression level and substrate affinity. Therefore, flux data in the present study was fitted to a previously developed modified Michaelis−Menten model that takes into account aqueous boundary layer resistance (eq 1). Data from sodium-free studies were fitted to a passive transport model (eq 2).

$$J = \frac{P_{ABL}\left(\frac{J_{max}}{K_t + S} + P_p\right)S}{P_{ABL} + \frac{J_{max}}{K_t + S} + P_p} \quad (1)$$

$$J = \frac{P_{ABL}P_pS}{P_{ABL} + P_p} \quad (2)$$

where J is taurocholate flux, J_{max} and K_t are the Michaelis−Menten constants for hASBT-mediated transport, S is taurocholate (i.e., substrate) concentration, P_p is the passive taurocholate permeability coefficient, and P_{ABL} is the aqueous boundary layer (ABL) permeability. In eqs 1 and 2, P_{ABL} was 70×10^{-6} cm/s.[10] Equations 1 and 2 were applied simultaneously to sodium-containing and sodium-free flux data to estimate K_t, J_{max}, and P_p. A pooled data analysis approach was used to model flux data from multiple occasions. Briefly, the pooled approach entailed fitting eqs 1 and 2 simultaneously to pooled flux data from all occasions, to yield a single K_t estimate for all occasions; J_{max} and P_p varied with occasion.

The following competitive inhibition model was applied to cis-inhibition studies of taurocholate uptake by individual bile acids:[10]

$$J_{ABL} = \frac{P_{ABL}\left(\frac{J_{max}}{K_t\left(1 + \frac{I}{K_i}\right) + S} + P_p\right)S}{P_{ABL} + \left(\frac{J_{max}}{K_t\left(1 + \frac{I}{K_i}\right) + S}\right) + P_p} \quad (3)$$

where I is the concentration of inhibitor (i.e., CDCA conjugate) and S is the concentration of taurocholate (i.e., 0.5 or 5 μM). In applying eq 3, only K_i was estimated. The other three parameters (i.e., J_{max}, K_t, and P_p) were estimated from taurocholate uptake studies without inhibitor using eqs 1 and 2, as described above where $P_{ABL} = 150 \times 10^{-6}$ cm/s.

Statistical Analysis. Nonlinear curve fitting was performed using WinNonlin 4.1 (Pharsight, Mountain View, CA). Results were analyzed using Student's t test and ANOVA. A p value of less than 0.05 was considered significant. The SEM of a ratio was calculated using the delta method.[11]

Results

Design of CDCA Conjugates with Varying Ionic and Steric Character around C-24. CDCA conjugates were designed to evaluate the influence of ionic character and steric bulk around the C-24 region. CDCA conjugates of glutamic acid or lysine were employed to yield congeneric series differing in charge (monoanionic, dianionic, cationic, neutral, and zwitterionic) and charge location (proximal or distal to C-24). The steric effect was evaluated using ester conjugates that varied in size of ester substituent and location (proximal and/or distal). Glutamate conjugates of CDCA provide a carboxyl group or groups that are ionized at pH above 5. Similarly, lysine conjugates of CDCA can provide a protonated amine at pH below 8. Also, the multiple sites of conjugation on each glutamic acid and lysine would allow either to function as a linker for coupling bile acid with drug candidates, directly extending these results to potential prodrug design.

Figure 1 illustrates the glutamate conjugates of CDCA. Glutamic acid CDCA amide (Glu-CDCA) carries two negative charges proximal and distal to C-24 (i.e., α and γ positions, respectively). Monoanionic conjugates contained either one proximal or one distal carboxylate, with the other carboxylate esterified with methyl or benzyl substituent. For neutral conjugates, each carboxylate was esterified with substituents varying in steric bulk.

Figure 2 illustrates the structure of lysine conjugates of CDCA. Unlike glutamate conjugates, lysine conjugates can provide a positive charge distal to C-24. The three lysine conjugates differed in ionic character. α-Lysine CDCA amide (Lys-CDCA) is zwitterionic with an α-carboxylate and ϵ-amino group. α-Lysine methyl ester CDCA amide (AM-lys-CDCA) is a cationic conjugate. α-Lysine(CBZ) benzyl ester CDCA amide (AB-Lys(Z)-CDCA) is neutral.

Synthesis of CDCA Conjugates. Most of the conjugates were synthesized with yields ranging from 60% to 90%. Identification of each of the synthesized conjugates was confirmed via ^{13}C NMR and MS. ^{13}C NMR spectra contained peaks consistent with the amide linkage and appropriate carbonyl chemistry. Coupling via the C-24 carboxylate of CDCA was checked by monitoring carboxylate shifts at

(10) Balakrishnan, A.; Polli, J. E. Deleterious effect of high transporter expression in the estimation of transporter kinetics. *AAPS J.* **2005**, *7*, R6224.

(11) Tanner, M. A. *Tools for Statistical Inference, vol. 67: Lecture Notes in Statistics*; Springer-Verlag: Berlin, 1992.

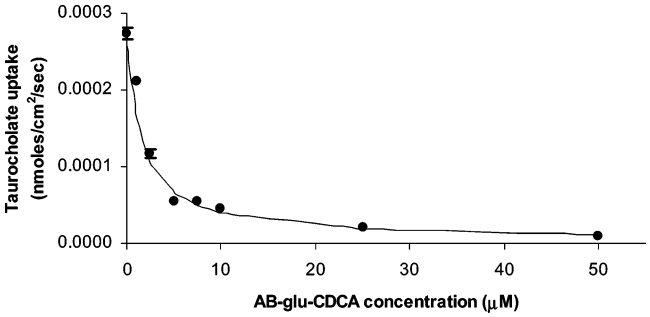

Figure 5. Concentration-dependent inhibition of taurocholate uptake into hASBT-MDCK monolayers by α-benzyl glutamic acid CDCA amide. α-Benzyl glutamic acid CDCA amide is abbreviated AB-glu-CDCA. Cis-inhibition studies of taurocholate uptake were carried out at varying concentrations of AB-glu-CDCA (0−50 μM). Closed circles indicate observed data points, while the solid line indicates model fitted data. Taurocholate uptake into hASBT-MDCK cells was reduced significantly by AB-glu-CDCA. Qualitatively similar profiles were observed for other CDCA conjugates.

∼180 ppm. MS data was consistent with the desired structures and a lack of bile acid in the final product. Purity for each of the conjugates was assessed by TLC, NMR, and LC−MS. TLC indicated a single spot for all the conjugates indicating high levels of conjugate purity. LC−MS quantified the level of CDCA impurity to be under 0.2%.

Inhibition Studies. Taurocholate uptake inhibition studies were carried out for each CDCA conjugate. Figure 5 illustrates the concentration-dependent inhibition of taurocholate uptake into hASBT-MDCK monolayers by α-benzyl glutamic acid CDCA amide (AB-glu-CDCA). AB-glu-CDCA inhibited taurocholate flux over 10-fold at 50 μM with a K_i of 0.55 μM. Similar profiles were observed for other CDCA conjugates. Dixon analysis of the monoanionic γ-methyl ester glutamic acid CDCA amide indicated a linear plot with an intercept not different from zero ($p > 0.05$), indicating competitive inhibition. Significant differences in inhibitory potencies were observed between the synthesized CDCA conjugates with K_i values ranging from 0.5 μM to greater than 1.5 M. The monoanionic CDCA conjugate, α-benzyl glutamic acid CDCA amide, exhibited the greatest potency, with a K_i of 0.55 μM. Dibenzyl glutamic acid CDCA amide and α-lysine(CBZ) benzyl ester CDCA amide exhibited negligible inhibitory potency, with K_i greater than 0.5 M.

Figure 6 illustrates the influence of C-24 ionic character on inhibition potency. Monoanionic, cationic, and neutral conjugates of CDCA exhibited high inhibitory potency (i.e., K_i lower than 10 μM). Both neutral and cationic conjugates exhibited high inhibition potency indicating that a negative charge is not essential for binding to hASBT. The dianionic Glu-CDCA exhibited poor inhibitory potency with a K_i greater than 100 μM. The zwitterionic Lys-CDCA exhibited moderate inhibition potency (i.e., K_i between 10 and 100 μM). Within monoanionic CDCA conjugates, conjugates with proximal (i.e., GM-glu-CDCA and GB-glu-CDCA) and

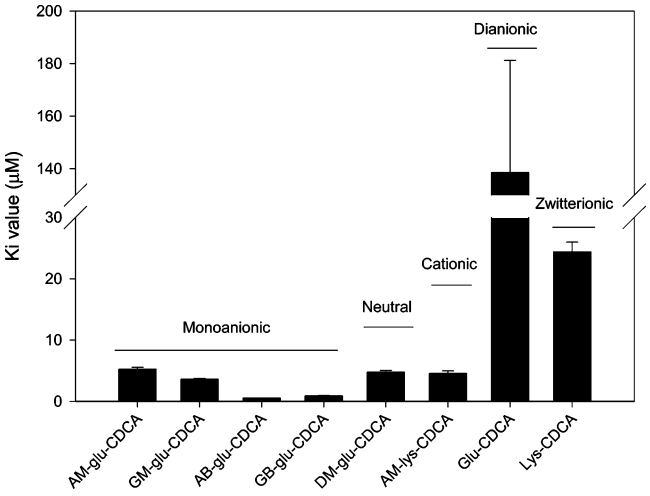

Figure 6. Effect of C-24 ionic character on inhibition potency. The inhibition potency of conjugates was influenced by ionic character around the C-24 region. Monoanionic, cationic, and neutral conjugates of CDCA exhibited high inhibitory potency (i.e., K_i lower than 10 μM). Within monoanionic CDCA conjugates, location of the negative charge proximal (GM-glu-CDCA and GB-glu-CDCA) or distal (AM-glu-CDCA and AB-glu-CDCA) to C-24 did not affect inhibitory activity. The dianionic Glu-CDCA exhibited poor inhibitory potency with a K_i greater than 100 μM. The zwitterionic Lys-CDCA exhibited moderate inhibition potency (i.e., K_i between 10 and 100 μM).

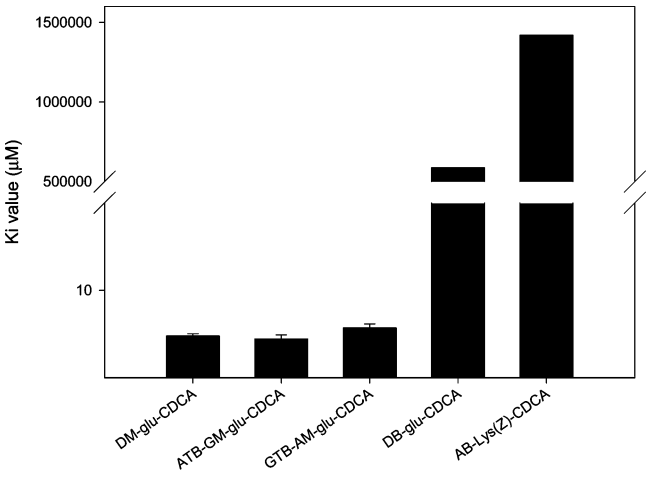

Figure 7. Effect of steric bulk around the C-24 region on inhibition potency of neutral conjugates. Compared to a methyl ester, a bulky *tert*-butyl ester proximal or distal to C-24 did not influence inhibition potency. However, the presence of two benzyl esters practically abolished interaction with hASBT (K_i > 0.5 M).

distal (i.e., GM-glu-CDCA and GB-glu-CDCA) negative charge exhibited similar inhibition potency. Meanwhile, each AB-glu-CDCA and GB-glu-CDCA exhibited K_i values that were 5-fold lower than those of the corresponding methyl ester conjugates.

Figure 7 illustrates the C-24 steric influence on the hASBT-inhibition potency of neutral conjugates. Compared to a methyl substituent, the presence of a *tert*-butyl group

Table 1. Kinetic Estimates of hASBT-Mediated Transport of CDCA Conjugates[a]

ionic character	conjugate	normalized J_{max}	K_t (μM)	P_p (cm/s) $\times 10^6$
dianionic	Glu-CDCA	nm[b]	nm	1.30 (0.09)
monoanionic	AM-glu-CDCA	1.28 (0.17)	3.92 (0.52)	1.89 (0.16)
	AB-glu-CDCA	0.923 (0.145)	0.249 (0.285)	5.32 (0.35)
	GM-glu-CDCA	1.97 (0.26)	7.79 (1.17)	1.45 (0.12)
	GB-glu-CDCA	2.06 (0.26)	0.149 (0.203)	2.03 (0.18)
cationic	AM-lys-CDCA	nm	nm	1.29 (0.09)
zwitterionic	Lys-CDCA	nm	nm	1.73 (0.14)
neutral	DM-glu-CDCA	nd[c]	nd	9.72 (0.29)

[a] Results are presented as mean (SEM) of at least three measurements. [b] Not measurable, i.e., not transported by hASBT. [c] Not determinable owing to high passive permeability.

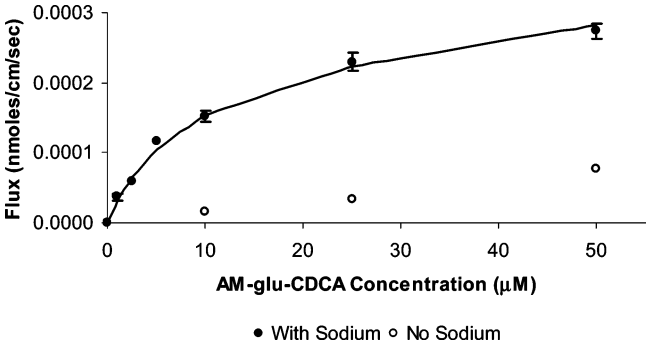

Figure 8. Concentration-dependent transport of α-methyl glutamic acid CDCA amide across hASBT-MDCK monolayers. AM-glu-CDCA flux was measured at varying concentrations (1−50 μM) in the presence and absence of sodium to delineate hASBT-mediated and passive flux components. Filled circles represent flux data in the presence of sodium. Open circles represent passive flux (i.e., absence of sodium). The solid lines represent the model fitted curve. AM-glu-CDCA transport in the presence of sodium was significantly larger than transport in the absence of sodium. Similar profiles were obtained for other monoanionic CDCA conjugates. Neutral conjugates of CDCA exhibited high passive flux, and active flux was not discerned.

distal or proximal to the C-24 region did not change the inhibitory potency of the conjugates. Additionally location of the *tert*-butyl group did not affect inhibitory potency as both ATB-GM-glu-CDCA and GTB-AM-CDCA exhibited similar K_i values. On the contrary, the presence of two benzyl groups completely abolishes inhibitory activity in the case of α,γ-dibenzyl ester glutamic acid CDCA amide.

Transport Studies. Inhibition data indicated most conjugates to generally exhibit good inhibition potency. However, substrate requirements for hASBT-mediated translocation may differ from requirements for hASBT inhibition. Subsequently, each conjugate exhibiting hASBT inhibition was evaluated for hASBT-mediated transport. Table 1 summarizes the kinetic parameters of hASBT-mediated transport for all the CDCA conjugates.

Figure 8 illustrates the concentration-dependent transport of α-methyl glutamic acid CDCA amide (AM-glu-CDCA) across hASBT-MDCK monolayers. Transport of AM-glu-CDCA was mediated largely by hASBT, with an approximately 12-fold greater flux from sodium-containing studies than from sodium-free studies. Similar profiles were obtained for the other three monoanionic conjugates of CDCA. The dianionic conjugate glutamic acid CDCA amide did not exhibit any hASBT-mediated transport, as can be expected from its poor inhibition potency. The cationic and the zwitterionic conjugate lysine conjugates did not exhibit significant hASBT-mediated transport, suggesting that these features abolish hASBT-mediated transport, in spite of their high inhibition potency. The neutral conjugate of glutamic acid α,γ-dimethyl glutamic acid CDCA amide (DM-glu-CDCA) did not show apparent hASBT-mediated transport, perhaps due to its high passive permeability.[12]

Overall, significant hASBT-mediated transport was observed only for monoanionic conjugates of CDCA. All the monoanionic conjugates were substrates for hASBT (Table 1). Within monoanionic CDCA conjugates, conjugates with either α- or γ-carboxylate exhibited similar substrate affinities indicating that the location of free carboxylate did not influence transport affinity. In comparing benzyl versus methyl esters, benzyl esters were more favored with approximately 10-fold lower K_t values. These results mirror the trends observed from inhibition studies, regarding the location of the free carboxylate and nature of the ester substituent (Figure 6).

Discussion

The human ileal bile acid transporter, also known as hASBT (SLC10A2), is a key component in the enterohepatic recirculation of bile acids and serves as a target to enhance oral drug absorption. Structural information on hASBT has been restricted to its primary sequence and membrane topology.[13] In the absence of a high-resolution crystal structure for hASBT, little is known about the interaction of hASBT with its substrates. This general lack of information has resulted in very few successful attempts at increasing bioavailability of compounds with poor intestinal permeability.[14,15]

Previous studies with native bile acids have indicated that C-24 conjugation enhances affinity to hASBT and results in enhanced hASBT-mediated transport.[6,16] However, it is not clear how C-24 chemistry influences interaction with hASBT.

(12) Lentz, K. A.; Polli, J. W.; Wring, S. A.; Humphreys, J. E.; Polli, J. E. Influence of passive permeability on apparent P-glycoprotein kinetics. *Pharm. Res.* **2000**, *17*, 1456−1460.

(13) Zhang, E. Y.; Phelps, M. A.; Banerjee, A.; Khantwal, C. M.; Chang, C.; et al. Topology scanning and putative three-dimensional structure of the extracellular binding domains of the apical sodium-dependent bile acid transporter (SLC10A2). *Biochemistry* **2004**, *43*, 11380−11392.

(14) Zhang, E. Y.; Knipp, G. T.; Ekins, S.; Swaan, P. W. Structural biology and function of solute transporters: implications for identifying and designing substrates. *Drug Metab. Rev.* **2002**, *34*, 709−750.

(15) Hagenbuch, B.; Dawson, P. The sodium bile salt cotransport family SLC10. *Pfluegers Arch.* **2004**, *447*, 566−570.

Previous studies by Lack et al. indicated that a negative charge around C-24 is essential for interaction with hASBT.[7] These studies were based on data from rat everted sac model, where bile acid transport was confounded with other intestinal transporters. Additionally, it was suggested that the negative charge should be distal to C-24. However, recent studies from our laboratory with neutral acyclovir conjugates indicated that neutral conjugates are transported via hASBT. A similar observation was also made by Swaan et al., suggesting that a hydrogen bond acceptor could substitute for the negative charge.[8] Results from Kramer et al. indicated that hybrids of bile acid and HMG CoA reductase inhibitors lacking a negative charge were able to inhibit taurocholate uptake in rabbit brush border membrane vesicles.[17,18] This lack of agreement between recent studies and Lack's earlier observations would appear to reflect the limitations of the assay system used in earlier studies. A recently developed hASBT-MDCK addressees some of these limitations and provides a convenient assay system for the assessment of hASBT function.[9]

The present study reveals insights about the influence of ionic character and steric bulk around the C-24 region of bile acid conjugates in governing interaction with hASBT. The influence of ionic character was studied systematically using CDCA conjugates of glutamic acid or lysine which varied in charge (monoanionic, dianionic, cationic, neutral, and zwitterionic) and charge location (proximal or distal to C-24). Steric effects were evaluated using conjugates of lysine and glutamate that varied in substituent bulkiness and location of the bulky substituent (proximal and/or distal). Glutamate and lysine conjugates were employed since they provide charged functional groups that can easily be derivatized to yield congeneric series of compounds varying in ionic and steric character.

Results from inhibition studies indicate that the presence of a single negative charge is not essential for binding to hASBT. Neutral and cationic CDCA conjugates exhibited potent inhibitory activity similarly to monoanionic conjugates. Zwitterionic conjugates also exhibited moderate inhibitory activity. The presence of two negative charges was detrimental to hASBT binding; dianionic conjugate glutamic acid CDCA amide exhibited very weak inhibitory activity. Table 2 compares the inhibition potency and substrate affinity of various CDCA conjugates. Interestingly, although the cationic conjugate (AM-lys-CDCA) and zwitterionic conjugate (Lys-CDCA) exhibited potent inhibitory activity, these conjugates were not substrates for hASBT. Only the monoanionic conjugates exhibited high hASBT-mediated transport, such that kinetic parameters could be estimated.

Table 2. C-24 Chemistry Effect on Inhibitory Potency and Transport Affinity[a]

ionic character	conjugate	inhibition potency[b]	substrate affinity[c]
dianionic	Glu-CDCA	low	nonsubstrate
monoanionic	AM-glu-CDCA	high	substrate
	AB-glu-CDCA	high	substrate
	GM-glu-CDCA	high	substrate
	GB-glu-CDCA	high	substrate
cationic	AM-Lys-CDCA	high	nonsubstrate
zwitterionic	Lys-CDCA	moderate	nonsubstrate
neutral	DM-glu-CDCA	high	nd[d]

[a] Inhibitory potency is classified as low, moderate, or high, depending on K_i. Transport affinity is characterized as substrates or nonsubstrates. [b] Low, moderate, and high potencies refer to $K_i > 100$ μM, 100 μM $> K_i >$ 10 μM, and $K_i <$ 10 μM, respectively. [c] A conjugate is classified as a substrate if the ratio of flux in the presence of sodium versus flux in absence of sodium is significantly greater than unity. [d] Not determinable owing to high passive permeability.

Previous studies have indicated that steric bulk influences hASBT-mediated transport. For example, transport of cholyl lysine fluorescein across ileum was relatively low and exhibited negligible differences in transport rate across jejunum and ileum. On the other hand, cholyl lysine NBD (nitrobenzoxadiazole) exhibited greater transport from the ileum compared to jejunum.[19] This difference in transport characteristics probably reflects the smaller size of NBD (nitrobenzoxadiazole) fluorophore compared to fluorescein. In the present study, the presence of a single bulky *tert*-butyl or benzyl substituent did not impede binding to hASBT. Additionally, location of the bulky substituent (i.e., proximal or distal to the C-24 carboxylate) did not influence inhibitory potency. However, the presence of two bulky groups practically abolished interaction with hASBT, as observed for α,γ-dibenzyl glutamic acid amide and α-lysine(CBZ) benzyl ester glutamic acid amide.

Results from the current study can be expected to facilitate future design of prodrugs targeting hASBT. From observed C-24 charge requirements, an appropriate linker can be used to achieve favorable C-24 chemistry space for the hASBT-mediated transport of prodrugs.

Abbreviations Used

hASBT, human apical sodium-dependent bile acid transporter; SLC, solute carrier family; MDCK, Madin-Darby canine kidney; HBSS, Hanks balanced salt solution; ABL, aqueous boundary layer; TCA, taurocholic acid; CDCA, chenodeoxycholic acid; Glu-CDCA, glutamic acid CDCA amide; AM-glu-CDCA, α-methyl glutamic acid CDCA amide; AB-glu-CDCA, α-benzyl glutamic acid CDCA

(16) Balakrishnan, A.; Wring, S. A.; Polli, J. E. Characterization of C-24 chemistry space and steroidal hydroxylation: Influence on bile interaction with hASBT. *AAPS J.* **2005**, *7*, R6223.

(17) Kramer, W.; Wess, G.; Enhsen, A.; Bock, K.; Falk, E.; et al. Bile acid derived HMG-CoA reductase inhibitors. *Biochim. Biophys. Acta* **1994**, *1227*, 137−154.

(18) Wess, G.; Kramer, W.; Han, X. B.; Bock, K.; Enhsen, A.; et al. Synthesis and biological activity of bile acid-derived HMG-CoA reductase inhibitors. The role of 21-methyl in recognition of HMG-CoA reductase and the ileal bile acid transport system. *J. Med. Chem.* **1994**, *37*, 3240−3246.

(19) Holzinger, F.; Schteingart, C. D.; Ton-Nu, H. T.; Eming, S. A.; Monte, M. J.; et al. Fluorescent bile acid derivatives: relationship between chemical structure and hepatic and intestinal transport in the rat. *Hepatology* **1997**, *26*, 1263−1271.

amide; GM-glu-CDCA, γ-methyl glutamic acid CDCA amide; GB-glu-CDCA, γ-benzyl glutamic acid CDCA amide; AM-lys-CDCA, α-lysine methyl ester CDCA amide; Lys-CDCA, α-lysine CDCA amide; DM-glu-CDCA, α,γ-dimethyl glutamic acid CDCA amide; ATB-GM-glu-CDCA, α-*tert*-butyl, γ-methyl glutamic acid CDCA amide; GTB-AM-glu-CDCA, γ-*tert*-butyl, α-methyl glutamic acid CDCA amide; DB-glu-CDCA, α,γ-dibenzyl glutamic acid CDCA amide; AB-Lys(Z)-CDCA, α-lysine(CBZ) benzyl ester CDCA amide.

Acknowledgment. This work was supported in part by National Institutes of Health Grant DK67530. A.C. is the recipient of an Independent Scientist Award (DA19634).

MP0600135